



Azithromycin-Ciprofloxacin-Impregnated Urinary Catheters Avert Bacterial Colonization, Biofilm Formation, and Inflammation in a Murine Model of Foreign-Body-Associated Urinary Tract Infections Caused by *Pseudomonas aeruginosa*

Hina Saini, Anitha Vadekeetil,  Sanjay Chhibber,  Kusum Harjai

Department of Microbiology, Panjab University, Chandigarh, India

ABSTRACT *Pseudomonas aeruginosa* is a multifaceted pathogen causing a variety of biofilm-mediated infections, including catheter-associated urinary tract infections (CAUTIs). The high prevalence of CAUTIs in hospitals, their clinical manifestations, such as urethritis, cystitis, pyelonephritis, meningitis, urosepsis, and death, and the associated economic challenges underscore the need for management of these infections. Biomaterial modification of urinary catheters with two drugs seems an interesting approach to combat CAUTIs by inhibiting biofilm. Previously, we demonstrated the *in vitro* efficacy of urinary catheters impregnated with azithromycin (AZM) and ciprofloxacin (CIP) against *P. aeruginosa*. Here, we report how these coated catheters impact the course of CAUTI induced by *P. aeruginosa* in a murine model. CAUTI was established in female LACA mice with uncoated or AZM-CIP-coated silicone implants in the bladder, followed by transurethral inoculation of 10^8 CFU/ml of biofilm cells of *P. aeruginosa* PAO1. AZM-CIP-coated implants (i) prevented biofilm formation on the implant's surface ($P \leq 0.01$), (ii) restricted bacterial colonization in the bladder and kidney ($P < 0.0001$), (iii) averted bacteriuria ($P < 0.0001$), and (iv) exhibited no major histopathological changes for 28 days in comparison to uncoated implants, which showed persistent CAUTI. Antibiotic implants also overcame implant-mediated inflammation, as characterized by trivial levels of inflammatory markers such as malondialdehyde ($P < 0.001$), myeloperoxidase ($P < 0.05$), reactive oxygen species ($P \leq 0.001$), and reactive nitrogen intermediates ($P < 0.01$) in comparison to those in uncoated implants. Further, AZM-CIP-coated implants showed immunomodulation by manipulating the release of inflammatory cytokines interleukin-6 (IL-6), tumor necrosis factor alpha (TNF- α), and IL-10 to the benefit of the host. Overall, the study demonstrates long-term *in vivo* effectiveness of AZM-CIP-impregnated catheters, which may possibly be a key to success in preventing CAUTIs.

KEYWORDS quorum sensing, urinary tract infection

Health care facilities employ various invasive devices like vascular or urinary catheters (UCs), ventilators, cardiac valves, and implants for medical procedures meant for the benefit of patients. However, infection of these very devices complicates the treatment of hospitalized patients, resulting in health care-associated infections (HAIs). Urinary tract infection (UTI) is one of the most common types of HAI, and around 75 to 80% of hospital-acquired UTIs are related to urinary catheterization (1). Urethral cath-

Received 2 September 2016 Returned for modification 20 September 2016 Accepted 12 December 2016

Accepted manuscript posted online 28 December 2016

Citation Saini H, Vadekeetil A, Chhibber S, Harjai K. 2017. Azithromycin-ciprofloxacin-impregnated urinary catheters avert bacterial colonization, biofilm formation, and inflammation in a murine model of foreign-body-associated urinary tract infections caused by *Pseudomonas aeruginosa*. Antimicrob Agents Chemother 61:e01906-16. <https://doi.org/10.1128/AAC.01906-16>.

Copyright © 2017 American Society for Microbiology. All Rights Reserved.

Address correspondence to Kusum Harjai, kusumharjai1961@gmail.com.

eters are indispensable devices that may be used in patients for a short term to collect urine during surgical interventions and orthopedic procedures and to measure urine output of ICU patients or for a long term to manage ureteral obstruction, urinary retention, and incontinence. The major risk in short- and long-term catheterization is the development of biofilm on the surface of the urinary catheter, which plays an important role in the pathogenesis of catheter-associated UTIs (CAUTIs). CAUTI is defined as a UTI in a patient with an indwelling urinary catheter in place at the time of or within 48 h prior to the onset of infection (1). The entry of bacteria into the bladder may occur by adherence to the urinary catheter surface during or after catheter insertion or by colonization of the catheter bag (3). Biofilm formation commences when bacteria attach to the catheter surface and/or uroepithelium and this adhesion is facilitated by the formation of a conditioning film on the catheter by deposition of host urinary components like proteins and electrolytes. This is followed by phenotypic changes in bacteria resulting in the production of exopolysaccharides that entrap and protect the bacteria. Subsequently, there is replication of the attached bacteria, recruitment of additional planktonic bacteria, and formation of microcolonies that eventually mature into biofilm. Cross talk between bacteria (quorum sensing [QS]) at threshold concentrations results in gene expression that regulates the formation and detachment of biofilm in addition to virulence factor production (4).

In a clinical setting, treatment of biofilm-associated infections represents a mammoth task, since the bacteria enclosed in an extracellular matrix are inherently protected from host defenses and are markedly tolerant to antimicrobial treatments (5). The management of these infections becomes difficult, especially when an opportunistic and drug-resistant pathogen like *Pseudomonas aeruginosa* is the etiological agent. *P. aeruginosa* and *Candida* species are pathogens frequently isolated from long-term-catheterized patients subjected to repeated dosage of antibiotics (6). In a recent study conducted in India, CAUTIs were reported to be the second most frequently detected infection in health care settings and *P. aeruginosa* as the single most causative organism of HAI (7). The prevalence of CAUTIs in health care settings adds to the economic burden and the sequelae of these infections (cystitis, pyelonephritis, bacteremia, urosepsis, prostatitis, epididymitis, septic arthritis, or meningitis) are associated with increased mortality.

To curtail the risk of CAUTIs, several strategies have been implemented in the past (8–10). Catheters coated with hydrogels/nitrofurazone, silver nanoparticles, or bacteriophages or the use of bacterial interference has shown some success in the management of CAUTIs for short-term-catheterized patients; however, these are still far from preventing long-term CAUTIs, especially in immunocompromised individuals. The CDC's recent annual report on HAIs states that there has been no change in the overall incidence of CAUTIs from 2009 to 2014, thus emphasizing the urgent need to develop alternatives to thwart such infections (1). Since the formation of biofilm on the catheter surface plays a major role in the pathogenesis of CAUTIs, one of the novel approaches to restrict CAUTIs may involve attenuation of QS (11). Disruption of QS by various agents, such as ginseng, furanones, garlic, and azithromycin, has been related to an improved host response and a significant reduction in *P. aeruginosa*-induced biofilm pneumonia in animal models (12, 13).

In a previous study, authors reported the development of a novel UC impregnated with a combination of azithromycin (AZM) and ciprofloxacin (CIP) (AZM-CIP implants), both of which exhibit anti-QS activity. These catheters yielded promising results *in vitro* in terms of antimicrobial and antifouling activity, sustained drug release, prolonged antimicrobial durability, and stable shelf life against *P. aeruginosa* (14). Since *in vivo* studies are deemed essential to establish the effectiveness of any agent, it becomes necessary to assess the efficacy of these catheters in a foreign-body-associated UTI model in animals. Here we report the evaluation of AZM-CIP-impregnated catheters during the course of CAUTIs induced by *P. aeruginosa*. This combination of antibiotics was chosen keeping in view their different modes of action, synergism, and antibiofilm activities (15).

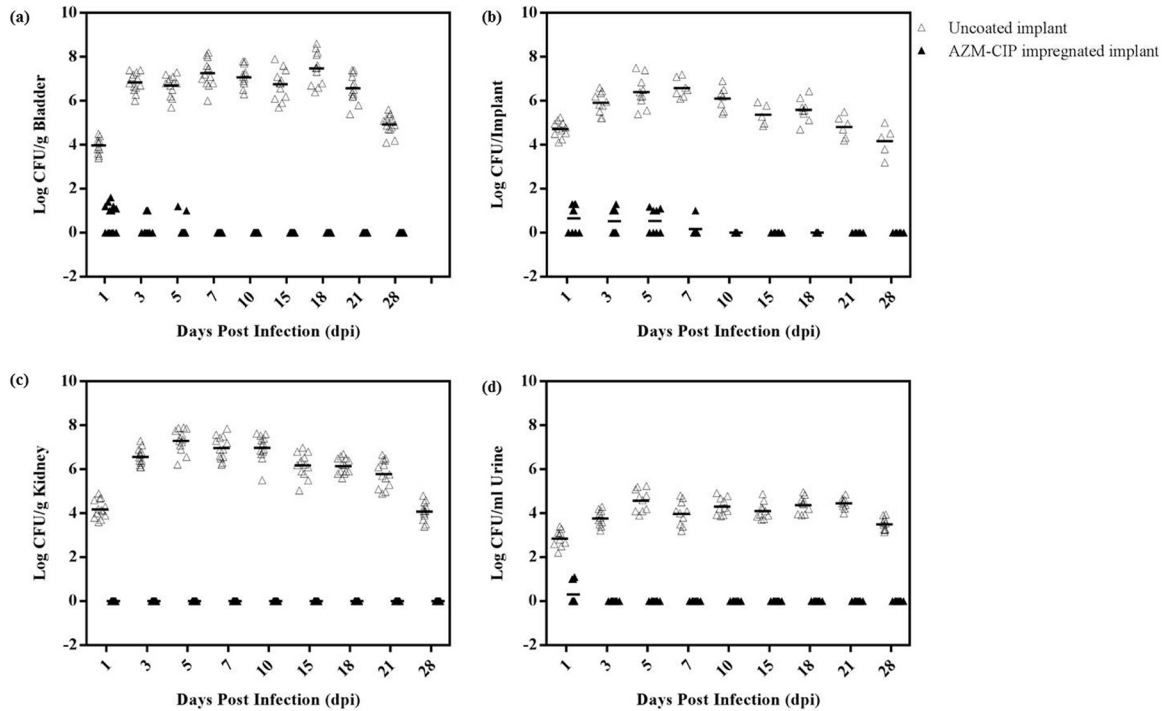


FIG 1 Bacteriological counts (log scale) in the bladders (a), implants (b), kidneys (c), and urine (d) of female LACA mice implanted with uncoated implants (Δ) or implants impregnated with a combination of azithromycin and ciprofloxacin (AZM-CIP) (\blacktriangle) and infected with *P. aeruginosa* PAO1. Each symbol represents the value for an individual mouse from three independent experiments with five mice for each group. A horizontal bar denotes the mean value for the respective groups. Mice with AZM-CIP implants showed resistance to bacterial colonization and biofilm formation on implants ($P \leq 0.01$) and in bladders ($P < 0.0001$), kidneys ($P < 0.0001$), and urine ($P < 0.0001$) in comparison to those of the uncoated implant group.

RESULTS

AZM-CIP implants thwart *P. aeruginosa* colonization and CAUTI establishment in comparison to uncoated implants. Bacteriological analyses of bladders, implants, kidneys, and urine were done on designated days postinfection (dpi) using animals with uncoated or AZM-CIP implants. Control mice treated with phosphate-buffered saline (PBS) did not show any bacterial burden on organs or implants or in urine (data not shown). The mean bladder bacterial load in mice with uncoated implants increased from a value of 4 log CFU/g on dpi 1 to 7.4 log CFU/g on dpi 18, with a subsequent reduction to 4.9 log CFU/g on dpi 28 (Fig. 1a). In contrast, animals with AZM-CIP implants showed an average of <1 log CFU/g of bladder bacteria until dpi 5, and no viable bacteria were recovered thereafter ($P < 0.0001$, versus uncoated implant group on all dpi). Nearly 59% and 57% of uncoated and AZM-CIP implants, respectively, were retrieved from the bladders. Silicone tubing implants provided a good surface for the adherence of bacteria, whereby consistent biofilm formation was observed on uncoated implants on all days with a mean bacterial recovery of 5.4 log CFU/implant (Fig. 1b). In contrast, the presence of AZM-CIP implants restricted bacterial colonization on their surfaces to <1 log CFU/implant until dpi 7; from that point on, no bacteria were recovered ($P \leq 0.01$). The ascending course of infection from the bladder to the kidney was ascertained by the recovery of bacteria from renal tissues of mice with uncoated implants. A mean renal bacterial count of 4.2 log CFU/g was observed on dpi 1, reaching a peak value of 7.5 log CFU/g by dpi 5 and decreasing thereafter to 4.1 log CFU/g on dpi 28 (Fig. 1c). It is noteworthy that bacteria remained confined to the bladder and could not be recovered from the kidneys of mice with antibiotic-impregnated implants ($P < 0.0001$). Bacteriuria was also assessed in the two groups (Fig. 1d): an average of 2.8 to 4.6 log CFU/ml of bacteria was present in the urine of mice with uncoated implants on all days, and <1 log CFU/ml of bacteria was recovered on dpi 1 from the antibiotic-impregnated implant group, with an absence of bacteria

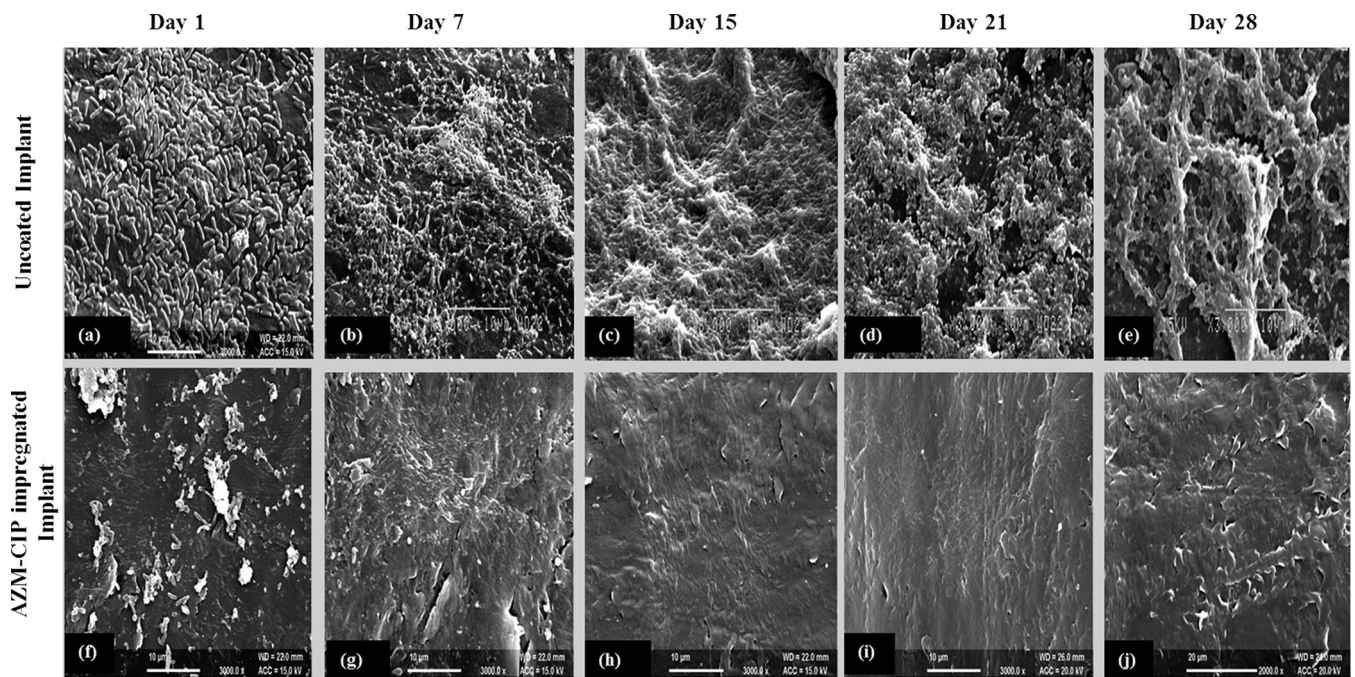


FIG 2 Scanning electron micrographs of uncoated implants (a to e) and AZM-CIP implants (f to j) retrieved on different days postinfection (dpi) from the bladders of female LACA mice infected with *P. aeruginosa* PAO1. Panels a to e suggest the successive progression of the formation of biofilm with a thick extracellular matrix on the surfaces of uncoated implants throughout the tested intervals. Panels f to j show the attachment of bacteria on dpi 1, followed by the absence of biofilm bacteria after dpi 7 until dpi 28 on the surfaces of AZM-CIP implants. Bars, 10 (a to i) and 20 (j) μ m.

thereafter ($P < 0.0001$). The bacteriology results suggest that AZM-CIP implants were proficient *in vivo* in battling bacterial adhesion, colonization, and subsequent biofilm formation, thus affecting the course of CAUTI, in comparison to the uncoated implants, which showed persistent colonization of bacteria on the implants and organs as well as shedding of bacteria in urine.

Antibiotic-impregnated implants prevent biofouling *in vivo*. The uncoated and antibiotic-coated implants retrieved from the bladders of mice at specified intervals were observed by scanning electron microscopy (SEM). The surfaces of uncoated implants showed attachment of a large number of rod-shaped bacteria, generation of biofilm on dpi 1 (Fig. 2a), and massive biofilm formation characterized by deep-seated bacteria in a dense extracellular matrix until dpi 28 (Fig. 2b to e). Conversely, AZM-CIP implants showed adherence of only a few bacterial cells on dpi 1 (Fig. 2f) and the complete absence of biofilm bacteria after dpi 7 (Fig. 2h to 2j). These findings indicate the effectiveness of AZM-CIP implants in hampering biofilm formation *in vivo* for about 28 days.

AZM-CIP implants induce mild inflammation, preventing severe edema in the bladder and tissue damage in the kidneys of animals. Histopathological changes in the bladders and kidneys of animals with uncoated or antibiotic-impregnated implants were viewed with a light microscope following staining of tissues with hematoxylin and eosin. On dpi 1, the bladders of animals with uncoated implants exhibited damage to the uroepithelium (Fig. 3a), with moderate inflammation in mucosa represented by infiltration of polymorphonuclear leukocytes (PMNLs) (Fig. 3b) (severity score [SS], 2), while the bladders of animals with AZM-CIP implants revealed disrupted and inflamed mucosa (Fig. 3c) showing clusters of leukocytes within the lamina propria (LP) (Fig. 3d), indicating inflammation (SS, 1). One week later, the bladders with uncoated implants became edematous (Fig. 3e) with increased neutrophil infiltration in the mucosal LP, indicating cystitis (SS, 3). However, the bladders with AZM-CIP implants showed increased vascularity, fibrous tissue (Fig. 3g), and excess cells in the LP (Fig. 3h) (SS, 1). From dpi 15 to 28, the bladders with uncoated implants showed a successive progres-

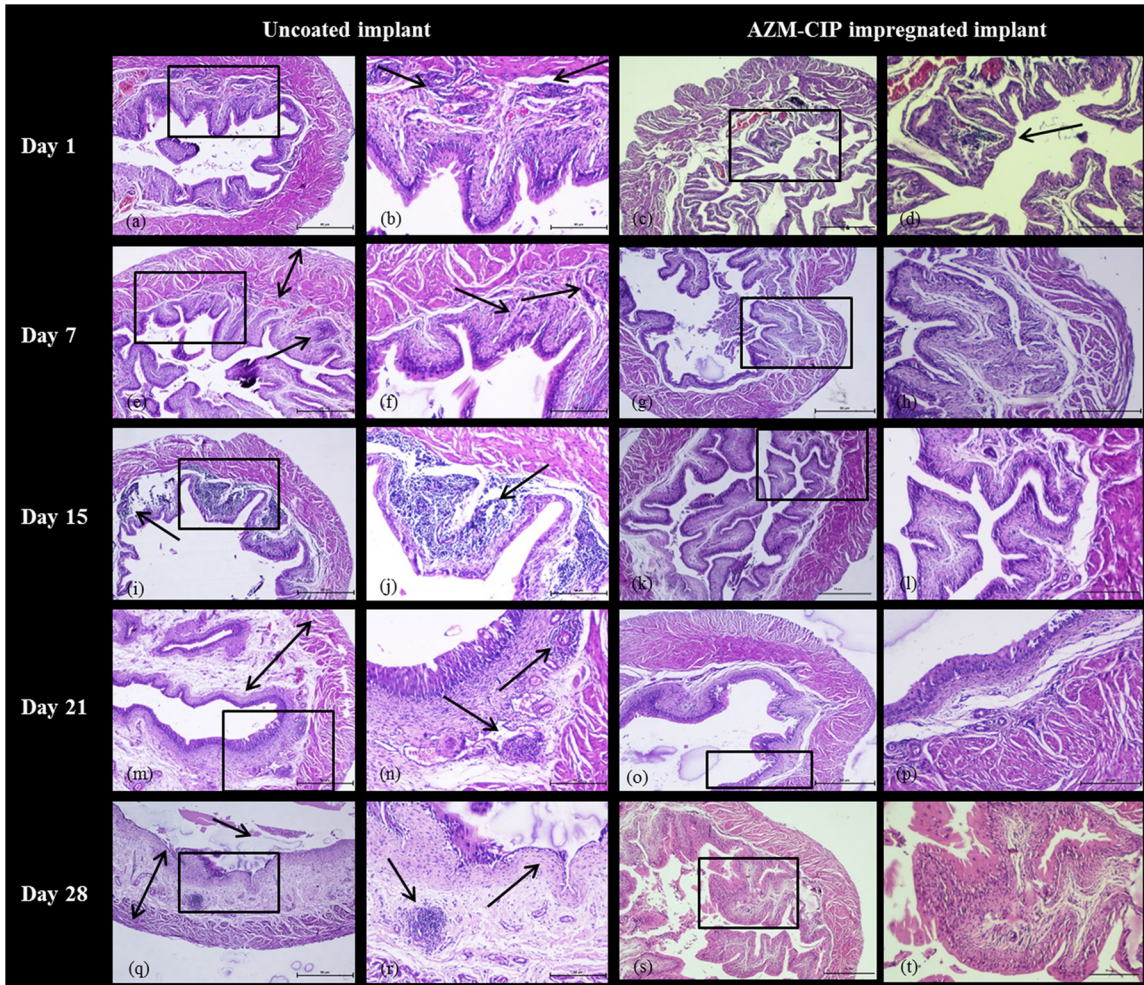


FIG 3 Histopathology micrographs of bladders derived at weekly intervals from female LACA mice implanted with uncoated or AZM-CIP-impregnated implants and infected with *P. aeruginosa* PAO1. The tissues were viewed at a magnification of $\times 40$ (a, c, e, g, i, k, m, o, q, and s) and $\times 100$ (b, d, f, h, j, l, n, p, r, and t) under a light microscope. A black box shows the area with or without distinct inflammatory changes in panels a, c, e, g, i, k, m, o, q, and s that are magnified in panels b, d, f, h, j, l, n, p, r, and t, respectively. Arrows indicate inflammatory changes such as the infiltration of neutrophils, and double-headed arrows indicate thickening of the muscularis propria. The bladders from mice in the uncoated implant group exhibit severe inflammation (e and f), massive infiltration of neutrophils (i and j), and ulceration and edema of the lamina propria (e, m, n, q, and r), whereas the bladders from mice in AZM-CIP implant group show initial inflammation and increased vascularity for 1 week, followed by no signs of inflammation. Bars, 50 μm .

sion of cystitis characterized by dense infiltration of lymphocytes in the LP (Fig. 3i and j) (SS, 4) and inflammation and edema of the mucosal LP, with increased vascularity and fibrosis (Fig. 3m), considerable lymphocytosis (Fig. 3n) (SS, 5), and finally signs of dilated bladder, ulcerated mucosa, marked inflammation, edema of the LP, and sloughing off of epithelium (Fig. 3q and r), thus leading to chronic cystitis (SS, 5). The bladders with antibiotic-impregnated implants showed signs of inflammation until dpi 7 (SS, 1); subsequently, normal tissue morphology was observed until dpi 28 (Fig. 3k, l, o, p, s, and t) (SS, 0). These results indicate that although AZM-CIP implants resulted in initial inflammation in the bladder tissue due to the normal host immune response to a foreign body, they prevented severe inflammation that results in chronic cystitis, as was seen with uncoated implants.

Histopathology images of kidney tissue on dpi 1 from animals with uncoated implants revealed inflammation near the renal pelvis with streaks of lymphocytes (Fig. 4a) and infiltration of neutrophils by displacement of the tubular spaces, suggestive of an ascending mode of infection (Fig. 4b) (SS, 8). By dpi 7, renal tissue showed lymphocytes in the lining of the kidney pelvis along with glomerular neutrophil

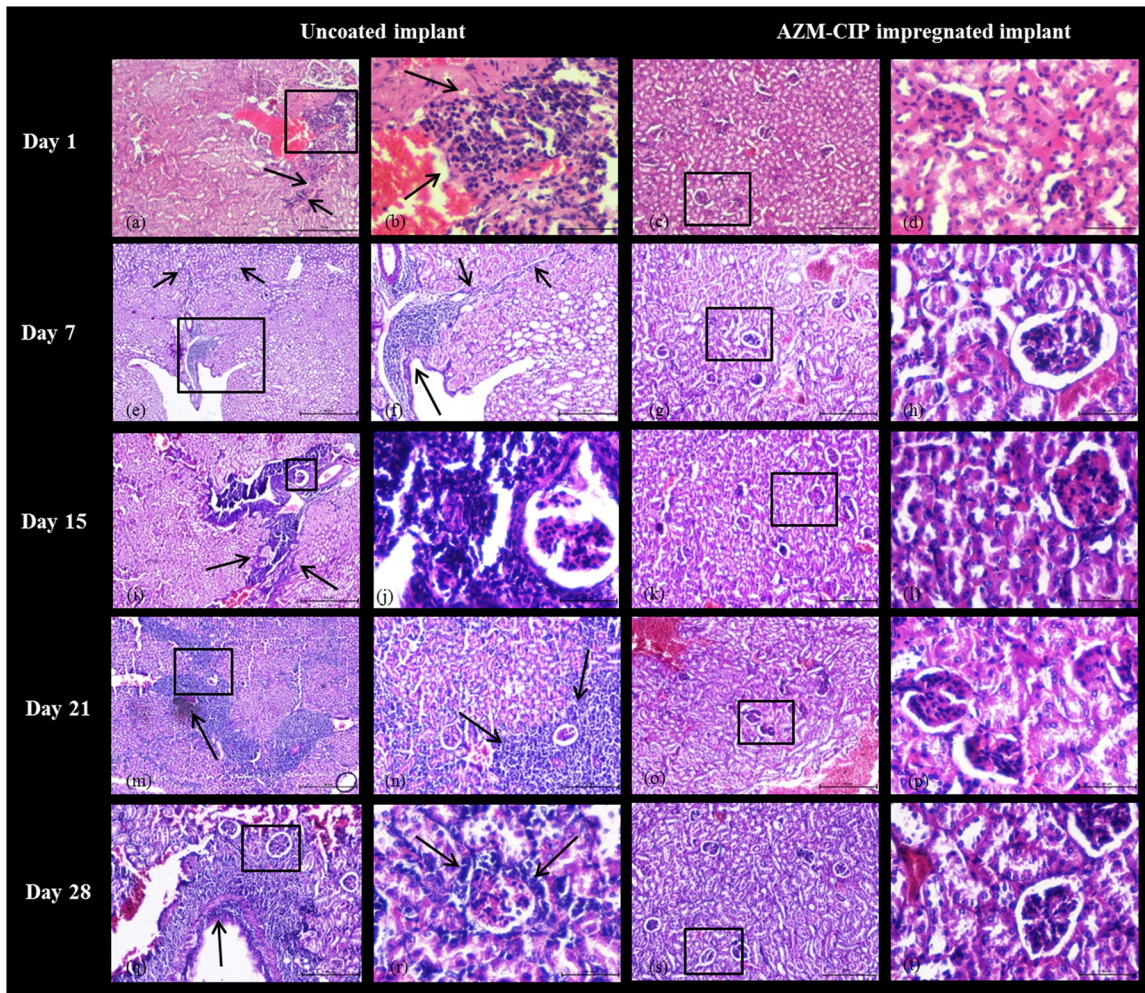


FIG 4 Histopathology micrographs of kidneys derived at weekly intervals from female LACA mice implanted with uncoated or AZM-CIP-impregnated implants and infected with *P. aeruginosa* PAO1. The tissues were viewed at magnifications of $\times 40$ (e, i, and m), $\times 100$ (a, c, f, g, k, n, o, q, and s), and $\times 400$ (b, d, h, j, l, p, r, and t) under a light microscope. A black box shows the area with or without distinct inflammatory changes in panels a, c, e, g, i, k, m, o, q, and s, which are magnified in panels b, d, f, h, j, l, n, p, r, and t, respectively. Arrows indicate inflammatory changes such as the infiltration of neutrophils. Renal tissues from the uncoated implant group reveal establishment of chronic pyelonephritis with severe inflammation in the renal pelvis (a and f), dense lymphocytic infiltration in the medulla (i), massive inflammation of the cortex with hemorrhage (m and n), and glomerular infiltration of neutrophils (r), whereas those from the AZM-CIP implant group show normal renal morphology at all intervals. Bars, 50 μm .

infiltration (Fig. 4e) and large streaks of inflammatory cells, indicating chronic interstitial inflammation (Fig. 4f) (SS, 11). Between 2 and 4 weeks, the architecture of the renal tissues was badly distorted, indicating the establishment of chronic pyelonephritis characterized by dense linear infiltrates of lymphocytes in the medullary region (Fig. 4i) and heavy neutrophil infiltration around the glomerulus (Fig. 4j) on dpi 15 (SS, 13); this was followed by heavy inflammation of the cortex region with hemorrhage that is suggestive of dense chronic inflammation (Fig. 4m and n) on dpi 21 (SS, 15), culminating in severe inflammation in the wall of the renal pelvis (Fig. 4q) and substantial infiltration of lymphocytes in the cortex around the glomerulus, indicating periglomerular inflammation (Fig. 4r) (SS, 16). In contrast, the kidneys of animals from the AZM-CIP implant group at all weekly intervals showed normal tissue morphology with normal tubules and glomeruli and no traces of inflammation. These results highlight the fact that antibiotic-coated catheters may prevent the establishment of pyelonephritis by restricting the ascent of bacteria from the bladder to the kidney.

Animals with uncoated implants show significantly higher levels of inflammatory markers in bladder and kidney. Bladder and kidney homogenates from animals

from both groups were assessed for the production of various inflammatory markers at specified intervals. Malondialdehyde (MDA), myeloperoxidase (MPO), reactive nitrogen intermediates (RNI), and superoxide dismutase (SOD) levels were observed to escalate in homogenates of both bladder and kidney tissues during the course of infection in the control group (Table 1). Alternatively, when tissue homogenates from the AZM-CIP implant group were tested, the MDA ($P < 0.001$), MPO ($P < 0.05$), RNI ($P < 0.001$), and SOD ($P \leq 0.001$) levels were significantly lower, indicative of a marked reduction in the release of these inflammatory markers. The data suggest that implantation of bladders with AZM-CIP implants arrested production in tissues of the inflammatory markers that were produced abundantly in the presence of uncoated implants.

AZM-CIP implants result in immunomodulation. Elevated levels of proinflammatory cytokines interleukin-6 (IL-6) and tumor necrosis factor alpha (TNF- α) were seen in the bladders and kidneys of mice with uncoated implants (Fig. 5a and b). However, the concentrations of the two cytokines assayed at weekly intervals were observed to be minimal in the bladder and renal homogenates of animals with antibiotic-coated implants ($P < 0.01$). In contrast, the levels of anti-inflammatory cytokine IL-10 were significantly higher in tissues from animals with antibiotic-coated implants at all tested intervals ($P < 0.01$) (Fig. 5c). These results indicate that the presence of AZM-CIP implants in the bladders of mice aid in controlling the disease process and inflammation by modulating the release of inflammatory cytokines to the benefit of the host.

DISCUSSION

Foreign-body-associated UTIs are one of the prominent device-related HAIs posing a great challenge to clinicians. The management of these infections becomes tougher when an opportunistic and drug-resistant pathogen like *P. aeruginosa* is the etiological agent. The pathogenesis of *P. aeruginosa*-mediated CAUTI is complex due to the formation of biofilms on the surfaces of UCs, which are hard to eradicate. To avert such infections, recent focus has shifted to local delivery systems employing a combination of agents to combat biofilm formation on devices. In a preliminary study, authors have demonstrated *in vitro* efficacy of a biomaterial generated by the impregnation of a UC with two drugs (AZM-CIP) (14). The present study evaluates the *in vivo* efficacy of an AZM-CIP-impregnated implant as a preventive strategy for CAUTIs caused by *P. aeruginosa*.

This study began with the establishment of an experimental CAUTI in order to effectively judge the performance of AZM-CIP implants. The course of the CAUTI was monitored for a month at designated time intervals postimplantation and postinoculation of *P. aeruginosa* biofilm cells in the bladders of animals with uncoated implants. The quantification of bacterial titers in bladders revealed persistent colonization with bacteria, indicating chronic cystitis. The number of bacteria present in the bladder correlated with the bacteria quantified from the retrieved implants at all tested intervals. Likewise, the bacteria were recovered in high titers from the kidneys of animals, confirming an ascending route of infection that led to chronic pyelonephritis. In addition, there was continuous shedding of bacteria in the urine of the mice. SEM images of uncoated implants retrieved from the bladder also showed substantial biofilm colonization for 28 days in which the bacteria were enclosed in a dense matrix. The bacteriological and microscopic findings suggest the persistence of bacteria in the urinary tracts of animals with uncoated implants for a month and perpetual biofilm formation on the implant surfaces representing the establishment of chronic UTIs. Similar findings were observed earlier, where persistent enterococcal cystitis was established in a murine model showing high titers of bacteria in the bladders and kidneys and biofilm production on silicone implant surfaces for 7 days (16).

Regardless of the heavy challenge with the biofilm cells (10^8 CFU/ml) of *P. aeruginosa*, insignificant bacterial titers were observed in the bladder as well as on the implants of animals harboring AZM-CIP implants. SEM imaging of antimicrobial-impregnated implants retrieved from the bladders revealed antibiofilm and antimicrobial properties, as evidenced by a small amount of biofilm on dpi 1 that showed

TABLE 1 Assessment of inflammatory markers in bladder and kidney tissue homogenates derived from animals with uncoated implants or AZM-CIP implants^a

dpi	MDA (nmol/mg protein)						RNI (μ mol/ml)						MPO (U/g)						SOD (mol/min)														
	Bladder		Kidney		Bladder		Kidney		Bladder		Kidney		Bladder		Kidney		Bladder		Kidney		Bladder		Kidney										
	Uncoated implant	AZM-CIP implant	Uncoated implant	AZM-CIP implant	Uncoated implant	AZM-CIP implant	Uncoated implant	AZM-CIP implant	Uncoated implant	AZM-CIP implant	Uncoated implant	AZM-CIP implant	Uncoated implant	AZM-CIP implant	Uncoated implant	AZM-CIP implant	Uncoated implant	AZM-CIP implant	Uncoated implant	AZM-CIP implant	Uncoated implant	AZM-CIP implant	Uncoated implant	AZM-CIP implant									
1	6.49 \pm 0.12	0.67 \pm 0.1	5.37 \pm 0.2	0.19 \pm 0.05	150.5 \pm 3.3	52.7 \pm 2.8	115.2 \pm 3	24.7 \pm 2.2	0.41 \pm 0.04	0.14 \pm 0.02	0.35 \pm 0.09	0.13 \pm 0.04	1.26 \pm 0.07	0.36 \pm 0.06	1.12 \pm 0.08	0.22 \pm 0.04	7	7.63 \pm 0.39	0.57 \pm 0.04	6.89 \pm 0.36	0.16 \pm 0.03	197.1 \pm 2.9	25.3 \pm 2.5	150.4 \pm 4.1	12.6 \pm 0.8	0.56 \pm 0.06	0.1 \pm 0.03	0.48 \pm 0.04	0.09 \pm 0.03	2.09 \pm 0.04	0.26 \pm 0.05	1.82 \pm 0.07	0.16 \pm 0.05
15	8.85 \pm 0.27	0.24 \pm 0.03	8.32 \pm 0.1	0.13 \pm 0.02	211.8 \pm 3.2	14.2 \pm 2.6	177.2 \pm 2.6	14.9 \pm 2.3	0.63 \pm 0.05	0.08 \pm 0.03	0.64 \pm 0.07	0.07 \pm 0.04	2.65 \pm 0.07	0.2 \pm 0.05	2.26 \pm 0.05	0.23 \pm 0.03	21	10.51 \pm 0.33	0.17 \pm 0.04	9.45 \pm 0.11	0.08 \pm 0.04	238.2 \pm 2.9	20.9 \pm 2.3	225.4 \pm 3.1	10.6 \pm 2.3	0.82 \pm 0.04	0.08 \pm 0.05	0.75 \pm 0.04	0.08 \pm 0.04	3.39 \pm 0.07	0.19 \pm 0.03	3.06 \pm 0.09	0.19 \pm 0.05
28	12.6 \pm 0.38	0.2 \pm 0.04	11.54 \pm 0.25	0.14 \pm 0.03	349.5 \pm 2.8	9.7 \pm 2	337.3 \pm 1.3	15 \pm 1.3	1.16 \pm 0.19	0.06 \pm 0.04	0.92 \pm 0.04	0.07 \pm 0.04	3.98 \pm 0.07	0.26 \pm 0.04	3.85 \pm 0.07	0.27 \pm 0.05	28	12.6 \pm 0.38	0.2 \pm 0.04	11.54 \pm 0.25	0.14 \pm 0.03	349.5 \pm 2.8	9.7 \pm 2	337.3 \pm 1.3	15 \pm 1.3	1.16 \pm 0.19	0.06 \pm 0.04	0.92 \pm 0.04	0.07 \pm 0.04	3.98 \pm 0.07	0.26 \pm 0.04	3.85 \pm 0.07	0.27 \pm 0.05

^aInflammatory markers included lipid peroxidation (malondialdehyde [MDA]), neutrophil response (myeloperoxidase [MPO]), reactive nitrogen species (reactive nitrogen intermediates [RNI]), and reactive oxygen species (superoxide dismutase [SOD]). There was a marked increase in the levels of all inflammatory markers from dpi 1 to 28 in tissues from mice in the uncoated implant group. Alternatively, homogenates from animals with antibiotic implants showed significant reductions in MDA ($P < 0.001$), MPO ($P < 0.05$), RNI ($P < 0.001$), and SOD ($P \leq 0.001$) on all dpi. Results are expressed as the mean \pm standard deviation.

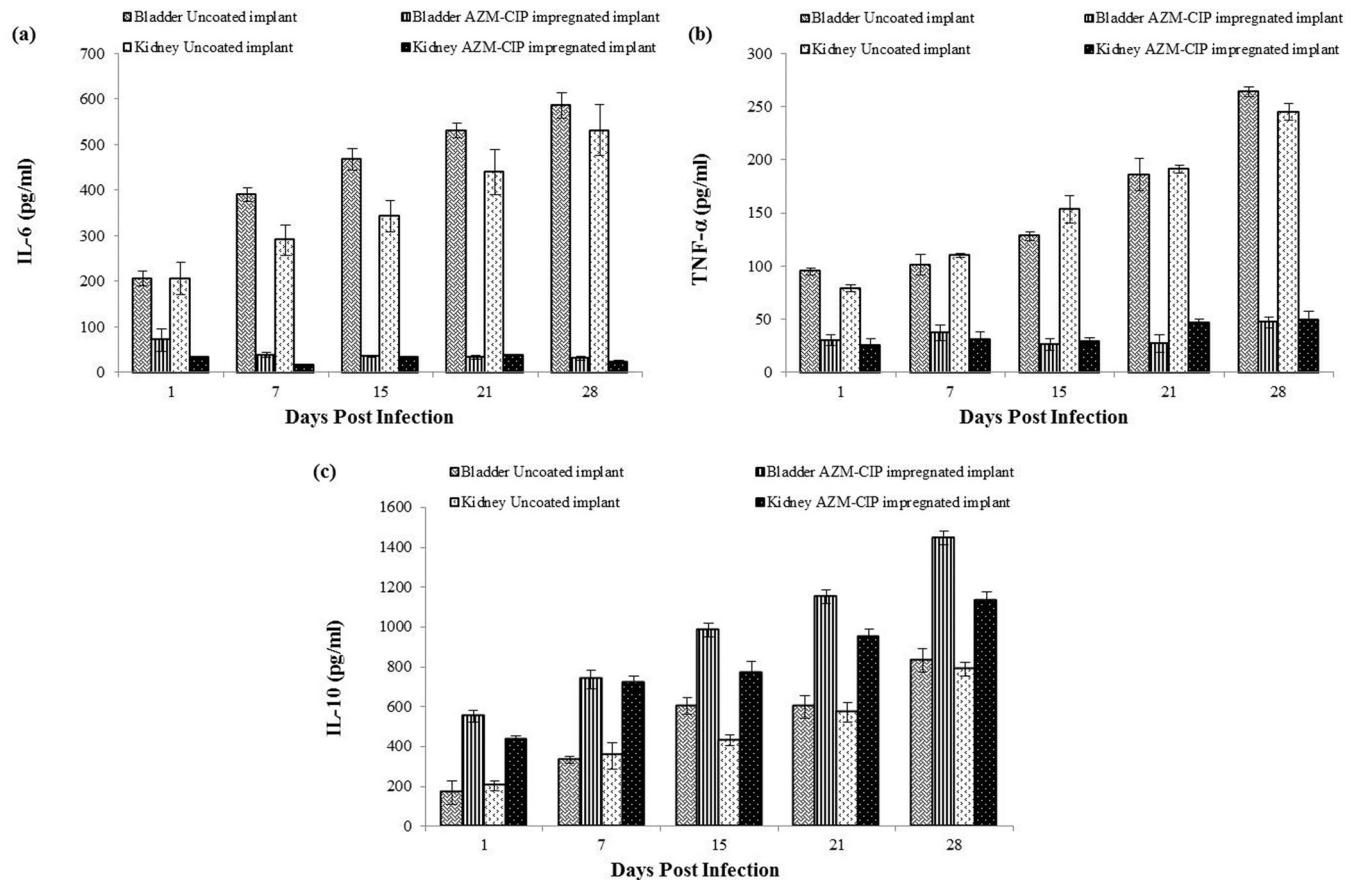


FIG 5 Quantification of proinflammatory cytokines IL-6 (a) TNF- α (b) and anti-inflammatory cytokine IL-10 (c) in the bladders and kidneys of *P. aeruginosa* PAO1-infected animals implanted with uncoated or AZM-CIP-impregnated implants. Decreased levels of IL-6 and TNF- α ($P < 0.01$) and elevated levels of IL-10 ($P < 0.01$) were found in animals in the AZM-CIP implant group compared to those of the animal group with uncoated implants.

complete eradication by dpi 7, possibly by the action of the two drugs released concomitantly from the implant surface. These findings indicate that antibiotic-coated catheters are capable of releasing drugs *in vivo* over a prolonged period at concentrations sufficient to kill the biofilm cells. In our previous study, the combination of macrolide and fluoroquinolone was proven effective in preventing bacterial colonization and subsequent biofilm formation *in vitro* for a long term (14). The striking feature of the present study is that the presence of AZM-CIP-impregnated UCs *in vivo* restricted the bacteria to the lower urinary tract and the kidneys remained sterile for the whole study period with absence of bacteriuria, hence highlighting the efficacy of these catheters in thwarting chronic UTIs. An earlier study revealed that Gendine-coated UCs prevented bacteriuria and invasive bladder infection in rabbits for 4 days, demonstrating good efficacy in preventing catheter-associated colonization of *Escherichia coli* in comparison with that of a silver-hydrogel-coated Foley's catheter and uncoated catheters (17). *In vivo* efficacy of antimicrobial CVCs was demonstrated for 30 days by Allan and colleagues, who showed that chlorhexidine-coated peripherally inserted central catheters significantly reduced *Staphylococcus aureus* colonization and prevented its migration in a rabbit model simulating a subcutaneous tunnel environment (18).

The clinical efficacy of AZM-CIP implants was demonstrated by histopathology. Although placement of AZM-CIP implants in the bladders resulted in foreign-body-mediated local inflammation attributed to the normal immune response of the host during the initial days of implantation, the severe inflammation seen in bladders with uncoated implants was overcome. The AZM-CIP implants were associated with negligible tissue pathology of the bladder, with no signs of the edema, lymphocytosis, or inflamed uroepithelium which were exhibited in bladders with uncoated implants. The

kidneys of animals with uncoated implants showed heavy periglomerular neutrophil infiltration, hemorrhage, and necrosis, indicating chronic pyelonephritis, whereas no histopathological changes were observed in the kidneys of animals with antimicrobial-coated implants. Other researchers have demonstrated the *in vivo* efficacy of novel antimicrobial hydroxyapatite nanoparticles in lowering the incidence of catheter-related bacteriuria, as evidenced by reduced biofilm formation and no histological changes in the uroepithelium in a CAUTI model of rabbits for 7 days (19).

Effective host defense against bacterial infection is dependent primarily on nonspecific antibacterial defense mechanisms which play an important role in the pathophysiology of *P. aeruginosa*-induced UTIs (20). In the present investigation, the various underlying mechanisms which resulted in a significant reduction in bacterial load and improved pathology with AZM-CIP implants were studied. During infection in animals with uncoated implants, there was a marked rise in the concentrations of inflammatory markers operative through the generation of MDA (lipid peroxidation), NO (reactive nitrogen intermediates), SOD (reactive oxygen species), and MPO (neutrophil recruitment); however, antimicrobial implants resulted in the suppression of these free radicals, hence minimizing the tissue damage. The foreign-body-induced trauma in the bladder tissues which was evident in the form of inflammation was measured by the levels of cytokines (IL-6, TNF- α , IL-10). AZM-CIP implants lowered the deleterious effects of implant-mediated inflammation, indicating immunomodulation and thus augmenting the host immune response toward infection. Upregulation of several inflammatory markers, such as IL-1 β , IL-6, IL-12, and IL-17, has been reported as a result of implantation of UCs in bladders followed by *Enterococcus faecalis* infection in a murine model of CAUTI (21).

There are numerous studies in the literature showing the *in vivo* activity of several antimicrobial and antiseptic catheters in preventing bacterial adhesion and biofilm formation on the surfaces of catheters (17–19, 22). However, the efficacy of all the catheters tested was limited to short-term catheterization (around 3 to 7 days). Fisher and coworkers demonstrated the efficacy of UCs impregnated with a combination of rifampin, sparflaxacin, and triclosan to prevent colonization by common uropathogens for 7 to 12 weeks in flow experiments conducted *in vitro*. Clinical trials are under way to establish the efficacy of this combination for both short-term and long-term catheterization (6). The success of AZM-CIP implants employed in the present study in preventing CAUTI *in vivo* may be attributed to (i) the inherent antimicrobial activity of the catheters, (ii) the dual drug therapy with different classes of antibiotics to avert development of antimicrobial resistance, (iii) the matrix loading or impregnation method chosen for coating both the external and internal surfaces with the drugs, thus preventing biofilm formation, (iv) the synergistic action of the drugs, and/or (iv) the ability to eradicate attached cells by the *in vivo* release of the drugs at effective concentrations (14, 15).

In view of the existing ineffective strategies against long-term CAUTIs, the present study suggests a ray of hope for clinicians in curbing the menace of one of the most challenging HAIs. To the best of our knowledge, this is the first report on long-term *in vivo* efficacy of a novel antimicrobial-impregnated silicone implant employing a combination of a macrolide and a flouroquinolone antibiotic against *P. aeruginosa*-induced CAUTIs. In conclusion, the present investigation draws the attention of researchers to effectively employ the combination of existing antibiotics to the benefit of CAUTI patients in the form of local delivery, such as with coated catheters, and to explore the role of these catheters in various disease models as well as against other uropathogens.

MATERIALS AND METHODS

Bacterial strain and growth conditions. *Pseudomonas aeruginosa* strain PAO1, originally procured from Barbara H. Iglewski (Department of Microbiology and Immunology, University of Rochester, USA) and maintained in our laboratory, was employed in the present study. The experiments were performed using an overnight culture of *P. aeruginosa* grown in Luria broth (HiMedia Laboratories Pvt. Ltd., Mumbai, India) under shaking conditions from a single colony grown on Luria agar plates. It was maintained as a glycerol stock (50%) and was stored at -20°C .

Biofilm. Biofilm cells were generated *in vitro* on a Rusch sterile Foley's catheter (Teleflex Medical GmbH, Kernen, Germany) as reported earlier (23). Fifty microliters of bacterial inoculum (about 1×10^8 CFU/ml) of 4-day-old biofilm cells scraped from the catheter surface was used for *in vivo* experiments.

Implant. Medical grade silicone tubing (SIL025) with specifications of 0.30 mm (inner diameter [i.d.]) by 0.64 mm (outer diameter [o.d.]) was procured (Braintree Scientific Inc., Braintree, MA, USA), and 4- to 6-mm segments of this tubing were used as implants in a murine model.

Antimicrobial-impregnated implant. Silicone implants comprising a combination of AZM (6%, wt/vol) (Cipla Limited, Goa, India) and CIP (3%, wt/vol) (HiMedia Laboratories Pvt. Ltd., Mumbai, India) were prepared using a solvent-based method as described previously (14). Briefly, separate solutions of AZM and CIP were prepared in different solvents. A 5-mg/ml concentration of NaOH (Thermo Fisher Scientific India Pvt. Ltd., Mumbai), an alkalinizing agent, was allowed to dissolve completely in methanol (Fisher Scientific) and dimethylformamide (Thermo Fisher Scientific India Pvt. Ltd., Mumbai) by stirring on a hot plate at 45°C, followed by the addition of AZM (6%, wt/vol) and CIP (3%, wt/vol), respectively, in small aliquots over 30 min to 1 h while stirring. The antimicrobial solutions of AZM and CIP were combined in the presence of ethyl acetate, a penetration agent, to facilitate complete penetration into the matrix. Four- to 6-mm segments of silicone tubing were immersed in the antimicrobial solution for 1 h; control implants were processed in the same manner but without antimicrobials. Subsequently, the implants were removed from the mixture and allowed to dry overnight at 37°C. They were rinsed with distilled water and allowed to dry for at least 2 h at room temperature before further testing.

Mouse strain and ethics statement. Female Swiss Webster (LACA) mice, 6 to 8 weeks old, weighing 20 to 30 g, bred and procured from Central Animal House, Panjab University, Chandigarh, India, were used in the study. The animals were housed in clean polypropylene cages and bedded with clean rice husk in a well-aerated room. Animals received standard pellets of antibiotic-free synthetic diet (M/s Ashirwad Industries Pvt. Ltd., Punjab, India) and water *ad libitum*. Animals were used after acclimatization to the new housing and experimental conditions for 1 to 2 weeks. All experimental protocols were approved by the Institutional Animal Ethics Committee of Panjab University, Chandigarh, India (approval no. IAEC/504) and performed in conformance with the guidelines of the Committee for the Purpose of Control and Supervision of Experiments on Animals (CPCSEA), Government of India.

Establishment of murine foreign-body-associated UTI. A chronic model for CAUTI was adapted with slight modifications (16). Briefly, a 4- to 6-mm-long segment of silicone tubing (SIL025) was mounted on top of 6- to 8-mm-long PE-10 polyethylene tubing (0.28-mm i.d. by 0.61-mm o.d.; BD Biosciences, San Jose, CA, USA), which was further attached to a Luer stub adapter. The whole assembly was rendered aseptic by immersion in 70% ethanol, air dried, and UV sterilized for about 2 h. The urethral area of each female LACA mouse was cleaned with absolute alcohol, and the bladder was emptied. The adapter with SIL025 and PE-10 tubing was gently inserted into the urethral opening of the mouse. PE-10 tubing was carefully advanced using forceps. SIL025 tubing was released into the bladder, and the adapter with PE-10 tubing was withdrawn carefully, thus leaving the silicone implant in the bladder. Following implantation of silicone tubing segments in the bladder, 50 μ l of PBS or biofilm cells of *P. aeruginosa* PAO1 (1×10^8 CFU/ml) were inoculated into the bladder via transurethral catheterization as described previously (24).

Animal groups. Mice were divided into two groups by allocating five mice/group/day of sacrifice, and the experiments were performed in triplicate. Group I was comprised of mice with uncoated implants and served as the infection control, whereas group II was comprised of mice with AZM-CIP implants for protection studies. All the animals were sacrificed at designated days postinfection by cervical dislocation.

Bacteriology. The bladders and kidneys from both groups were excised and processed under aseptic conditions on different dpi. Silicone implants were retrieved from the bladders of the animals whenever present. Bacteria were detached from the implants by sonication in PBS (0.1 M, pH 7.2) for 15 to 20 min at 50 Hz (Sonics and Materials Inc., CT, USA) and subsequently vortexed. Urine was collected from individual animals from both groups before sacrifice at designated time intervals. The quantitative bacterial loads (CFU) on implants and in tissues and urine were determined following serial dilution and spread plating on MacConkey agar. The plates were incubated at 37°C for 18 h to 24 h, and bacterial counts were performed.

SEM. Implants retrieved at different dpi from the bladders of animals were preserved in cold acetone after being rinsed with PBS. The implants were prepared for scanning electron microscopy (SEM) (JSM-6100; JEOL, Tokyo, Japan) by fixing them in 2.5% glutaraldehyde, followed by dehydration in different grades of ethanol (50 to 100%).

Histopathology. Bladder and kidney tissues of mice from both groups were fixed in 10% buffered formal saline and dehydrated in an ethanol gradient (30 to 100%). Tissues were then embedded in wax, sectioned, stained with hematoxylin and eosin, and viewed under a light microscope. Tissues from both groups were evaluated for histopathological changes on the basis of semiquantitative scoring. Severity scoring of bladder tissue was performed using a semiquantitative scale of 0 to 5 (25). The medulla, cortex, calyx, and subcalyx of each kidney were assessed using semiquantitative scores of 0 to 4. The individual scores of these four kidney sections were then summed to give a final severity score for the kidney, which ranged from 0 to 16 (26).

Assessment of inflammatory markers. Bladder as well as kidney tissue homogenates from the two animal groups were centrifuged at $1,500 \times g$ for 10 min. The supernatant was collected, passed through a 0.45- μ m filter (Pall Life Sciences, San Diego, CA, USA), and stored at -20°C until the time of the assay. The experiments were performed in triplicate.

MDA estimation. Tissue homogenate supernatants were mixed with an equal amount of Tris HCl (0.1 M, pH 7.4) and incubated at 37°C for 2 h. Subsequently, 10% (wt/vol) of ice-cold trichloroacetic acid (CDH, New Delhi, India) was added to the homogenates and centrifuged at $112 \times g$ for 10 min. The supernatant was mixed with 0.67% (wt/vol) thiobarbituric acid (HiMedia Laboratories Pvt. Ltd., Mumbai, India) and kept in a boiling water bath for 10 min. After cooling, the absorbance was measured at 532 nm, and the results were expressed as the amount of malondialdehyde (MDA) produced in nanomoles per milligram of protein (27).

Assessment of neutrophil response. Tissue neutrophils were quantified using a myeloperoxidase (MPO) assay. Bladders and kidneys were homogenized in 50 mM potassium phosphate buffer (pH 6.0) with 5% hexadecyl-trimethylammonium bromide (Fluka Chemie AG, Buchs, Switzerland) and 5 mM EDTA. Homogenates were sonicated and centrifuged at $4,000 \times g$ for 15 min. Supernatants were mixed with assay buffer (1:15), and absorbance was measured at 490 nm for 2 min. MPO units were calculated as 10 times the change in absorbance per minute per volume of supernatant per weight of tissue taken (28).

Estimation of reactive nitrogen intermediates (RNI). Nitric oxide (NO) production was estimated in tissue homogenate supernatants by mixing them with PBS, Griess reagent (Sigma-Aldrich Chemical Co. Ltd., St. Louis, MO, USA), and trichloroacetic acid. The mixture was then centrifuged for 15 min at $8,000 \times g$, and the absorbance of the supernatant was measured at 540 nm (29). NO levels were expressed in micromoles per milliliter.

Measurement of reactive oxygen species (ROS). Superoxide radical production in tissues was determined by estimating the amount of an antioxidant enzyme superoxide dismutase (SOD). Solution A (0.1 mM EDTA containing 50 mM Na_2CO_3), solution B (90 μg nitroblue tetrazolium [NBT]; HiMedia Laboratories Pvt. Ltd., Mumbai, India), solution C (0.6% Triton X-100 in solution A), and solution D (20 mM hydroxylamine hydrochloride; HiMedia Laboratories Pvt. Ltd., Mumbai, India) were added to the supernatants of homogenate. The rate of reduction of NBT was recorded, and the results were expressed as moles per minute (30).

Immunoassay for cytokine quantitation. Mouse IL-6, TNF- α , and IL-10 cytokines were quantitated in tissue homogenate supernatants per the manufacturer's protocol using ELISA kits (Krishgen Biosystems, Whittier, CA, USA), and results were expressed as picograms per milliliter. The experiments were done in triplicate.

Statistical methods. The data were analyzed statistically by a paired *t* test using GraphPad Prism v.6.07 (GraphPad Software Inc., La Jolla, CA). A *P* value of <0.05 was considered significant.

ACKNOWLEDGMENTS

We thank Mohinder Singh at Sophisticated Analytical Instrumentation Facility (SAIF), Panjab University, Chandigarh, India, for technical assistance with the scanning electron microscopy work and B. N. Datta (retired pathologist; PGIMER, Chandigarh, India) for analysis and interpretation of the tissue histopathology. We are grateful to Jaspal Singh for proofreading the manuscript.

This work was funded by the University Grants Commission, New Delhi, India, under the scheme of the Maulana Azad National Fellowship for Minority Students [F1-17.1/2013-2014/MANF-2013-14-SIK-CHA-22060/(SA-III/Website)].

REFERENCES

1. CDC. 2015. Catheter-associated urinary tract infections (CAUTI). CDC, Atlanta, GA. http://www.cdc.gov/HAI/ca_uti/uti.html.
2. Reference deleted.
3. Barford JMT, Coates ARM. 2009. The pathogenesis of catheter-associated urinary tract infection. *J Infect Prevention* 10:50–56. <https://doi.org/10.1177/1757177408098265>.
4. Jacobsen SM, Stickler DJ, Mobley HLT, Shirtliff ME. 2008. Complicated catheter-associated urinary tract infections due to *Escherichia coli* and *Proteus mirabilis*. *Clin Microbiol Rev* 21:26–59. <https://doi.org/10.1128/CMR.00019-07>.
5. Trautner BW, Darouiche RO. 2004. Role of biofilm in catheter-associated urinary tract infection. *Am J Infect Control* 32:177–183. <https://doi.org/10.1016/j.ajic.2003.08.005>.
6. Fisher LE, Hook AL, Ashraf W, Yousef A, Barrett DA, Scurr DJ, Chen X, Smith EF, Fay M, Parmenter CDJ, Parkinson R, Bayston R. 2015. Biomaterial modification of urinary catheters with antimicrobials to give long-term broadspectrum antibiofilm activity. *J Control Release* 202:57–64. <https://doi.org/10.1016/j.jconrel.2015.01.037>.
7. Dasgupta S, Das S, Chawan NS, Hazra A. 2015. Nosocomial infections in the intensive care unit: incidence, risk factors, outcome and associated pathogens in a public tertiary teaching hospital of Eastern India. *Indian J Crit Care Med* 19:14–20. <https://doi.org/10.4103/0972-5229.148633>.
8. Darouiche RO, Thornby JI, Cerra-Stewart C, Donovan WH, Hull RA. 2005. Bacterial interference for prevention of urinary tract infection: a prospective, randomized, placebo-controlled, double-blind pilot trial. *Clin Infect Dis* 41:1531–1534. <https://doi.org/10.1086/497272>.
9. Ha US, Cho YH. 2006. Catheter-associated urinary tract infections: new aspects of novel urinary catheters. *Int J Antimicrob Agents* 28:485–490. <https://doi.org/10.1016/j.ijantimicag.2006.08.020>.
10. Hooton TM, Bradley SF, Cardenas DD, Colgan R, Geerlings SE, Rice JC, Sanjay S, Anthony JS, Paul AT, Peter T, Lindsay EN. 2010. Diagnosis, prevention, and treatment of catheter-associated urinary tract infection in adults: 2009 International Clinical Practice Guidelines from the Infectious Diseases Society of America. *Clin Infect Dis* 50:625–663. <https://doi.org/10.1086/650482>.
11. Stickler DJ, Morris NS, McLean RJC, Fuqua C. 1998. Biofilms on indwelling urethral catheters produce quorum sensing signal molecules in situ and in vitro. *Appl Environ Microbiol* 64:3486–3490.
12. Hoffmann N, Lee B, Hentzer M, Rasmussen TB, Song Z, Johansen HK, Givskov M, Høiby N. 2007. Azithromycin blocks quorum sensing and alginate polymer formation and increases the sensitivity to serum and stationary-growth-phase killing of *Pseudomonas aeruginosa* and attenuates chronic *P. aeruginosa* lung infection in *Cftr*^{-/-} mice. *Antimicrob Agents Chemother* 51:3677–3687. <https://doi.org/10.1128/AAC.01011-06>.
13. Song Z, Kong KF, Wu H, Maricic N, Ramalingam B, Priestap H, Schnepfer L, Quirke JME, Høiby N, Mathee K. 2010. Panax ginseng has anti-infective activity against opportunistic pathogen *Pseudomonas aeruginosa* by inhibiting quorum sensing, a bacterial communication process critical

- for establishing infection. *Phytomedicine* 17:1040–1046. <https://doi.org/10.1016/j.phymed.2010.03.015>.
14. Saini H, Chhibber S, Harjai K. 2016. Antimicrobial and antifouling efficacy of urinary catheters impregnated with a combination of macrolide and fluoroquinolone antibiotics against *Pseudomonas aeruginosa*. *Biofouling* 32:795–806.
 15. Saini H, Chhibber S, Harjai K. 2015. Azithromycin and ciprofloxacin: a possible synergistic combination against *Pseudomonas aeruginosa* biofilm-associated urinary tract infections. *Int J Antimicrob Agents* 45:359–367. <https://doi.org/10.1016/j.ijantimicag.2014.11.008>.
 16. Guiton PS, Hung CS, Hancock LE, Caparon MG, Hultgren SJ. 2010. Enterococcal biofilm formation and virulence in an optimized murine model of foreign body-associated urinary tract infections. *Infect Immun* 78:4166–4175. <https://doi.org/10.1128/IAI.00711-10>.
 17. Hachem R, Reitzel R, Borne A, Jiang Y, Tinkey P, Uthamanthil R, Chandra J, Ghannoum M, Raad I. 2009. Novel antiseptic urinary catheters for prevention of urinary tract infections: correlation of in vivo and in vitro test results. *Antimicrob Agents Chemother* 53:5145–5149. <https://doi.org/10.1128/AAC.00718-09>.
 18. Allan ND, Giare-Patel K, Olson ME. 2012. An in vivo rabbit model for the evaluation of antimicrobial peripherally inserted central catheter to reduce microbial migration and colonization as compared to an uncoated PICC. *J Biomed Biotechnol* 2012:921617.
 19. Evliyaoglu Y, Kobaner M, Celebi H, Yelsel K, Dogan A. 2011. The efficacy of a novel antibacterial hydroxyapatite nanoparticle-coated indwelling urinary catheter in preventing biofilm formation and catheter-associated urinary tract infection in rabbits. *Urol Res* 39:443–449. <https://doi.org/10.1007/s00240-011-0379-5>.
 20. Mittal R, Sharma S, Chhibber S, Harjai K. 2008. Contribution of free radicals to *Pseudomonas aeruginosa* induced acute pyelonephritis. *Microb Pathog* 45:323–330. <https://doi.org/10.1016/j.micpath.2008.08.003>.
 21. Guiton PS, Hannan TJ, Ford B, Caparon MG, Hultgren SJ. 2013. *Enterococcus faecalis* overcomes foreign body-mediated inflammation to establish urinary tract infections. *Infect Immun* 81:329–339. <https://doi.org/10.1128/IAI.00856-12>.
 22. Darouiche RO, Mansouri MD, Zakarevicz D, AlSharif A, Landon GC. 2007. In vivo efficacy of antimicrobial-coated devices. *J Bone Joint Surg* 89:792–797.
 23. Bala A, Kumar R, Harjai K. 2011. Inhibition of quorum sensing in *Pseudomonas aeruginosa* by azithromycin and its effectiveness in urinary tract infections. *J Med Microbiol* 60:300–306. <https://doi.org/10.1099/jmm.0.025387-0>.
 24. Mittal R, Chhibber S, Sharma S, Harjai K. 2004. Macrophage inflammatory protein-2, neutrophil recruitment and bacterial persistence in an experimental mouse model of urinary tract infection. *Microbes Infect* 6:1326–1332. <https://doi.org/10.1016/j.micinf.2004.08.008>.
 25. Hopkins WJ, Gendron-Fitzpatrick A, Balish E, Uehling DT. 1998. Time course and host responses to *Escherichia coli* urinary tract infection in genetically distinct mouse strains. *Infect Immun* 66:2798–2802.
 26. Garg UC, Ganguly NK, Sharma S. 1987. Quantitative histopathological method for the evaluation of experimental ascending pyelonephritis. *Med Sci Res* 15:367–368.
 27. Anjaneyulu M, Chopra K. 2004. Effect of irbesartan on the antioxidant defence system and nitric oxide release in diabetic rat kidney. *Am J Nephrol* 24:488–496. <https://doi.org/10.1159/000080722>.
 28. Hang L, Haraoka M, Agace WW, Leffler H, Burdick M, Strieter R, Svanborg C. 1999. Macrophage inflammatory protein-2 is required for neutrophil passage across the epithelial barrier of the infected urinary tract. *J Immunol* 162:3037–3044.
 29. Rockett KA, Awburn MM, Rockett EJ, Cowden WB, Clark IA. 1994. Possible role of nitric oxide in malarial immunosuppression. *Parasite Immunol* 16:243–249. <https://doi.org/10.1111/j.1365-3024.1994.tb00346.x>.
 30. Imamura M, Aoki N, Saito T, Ohno Y, Maruyama Y, Yamaguchi J, Yamamoto T. 1986. Inhibitory effects of antithyroid drugs on oxygen radical formation in human neutrophils. *Acta Endocrinol* 112:210–216.